CHAPTER 284

THREE-DIMENSIONAL HYDRODYNAMICS ON A BARRED BEACH

Tae-Myoung Oh[1] and Robert G. Dean[2]

ABSTRACT

Results are described from fixed bed wave tank tests to examine the generation and existence of three-dimensional flows on a barred beach. All tests were carried out with the use of two-dimensional and three-dimensional bar, which represented periodic forms parallel to the coast superimposed on a linear sloping beach. For these tests, wave heights and wave direction fields within and adjacent to the surf zone were documented to calculate the wave-induced horizontal torque based on mean vorticity and momentum equations. The circulation pattern clearly demonstrated that rip currents were stable on a three-dimensionally barred beach. It was found that the individual component including the depth gradients in the longshore direction, i.e., the effects of the bar morphology, tended to stabilize the bar-induced celluar circulation on the three-dimensional beach morphology although increased momentum fluxes of waves in the area with opposing currents induced by the bar tended to exert a counter force against them. It appeared that the mass transport over the more elevated portions of the bar tended to return to offshore through the deeper portions of the bar, where the depth gradients in the longshore direction existed. The cause is believed to be due to the greater hydraulic efficiency of flows through deeper portions of the profile.

[1]Research Director, Woobo Space Co., Ltd., Seongkok Bldg. 7FL., #823-22 Yeoksam-Dong, Kangnam-Ku, Seoul, Korea, Zip-Code 135-080

[2]Professor, Coastal and Oceanographic Engineering Department, University of Florida, Gainesville, Fl 32611

INTRODUCTION

There are several proposed mechanisms to explain the presence of three- dimensional forms that are fairly regular and generally associated with rip currents, which range from the relatively simple to the complex, including: (1) Instability between the hydrodynamics and sedimentary systems (Hino, 1974; Deigaard, 1990), (2) Interaction beween waves and currents (Dalrymple and Losano, 1978), (3) Interaction between synchronous edge waves and incident waves (Bowen, 1969; Bowen and Inman, 1969), (4) Intersecting wave trains (Dalrymple, 1975), and (5) Structural controls by natural and/or constructed features (Gourlay, 1976; Wind and Vreugdenhil, 1986). Some of those mechanisms (Hino, 1974; Dalrymple and Losano, 1978) contended that rip currents in nature could be explained by the reinforcement of three-dimensional flows over two-dimensional morphology. However, previous laboratory investigations (Dean and Oh, 1994) suggested that rip currents were neither self-reinforcing nor stable on two-dimensional topography due to the stabilizing wave-induced torque associated with the increased momentum fluxes in the vicinity of seaward mass return flow; hence, substantial rip currents could not occur without the presence of a rip channel.

This paper comprises the results of a series of fixed bed wave tank experiments conducted on a barred beach to examine the effects of three-dimensional bar morphology on the tendency for celluar circulation inside the surf zone, thus discussing the questions including: (1) Rip currents of significant strength can form on a barred beach, and (2) Whether the interaction between rips and incident waves causes increased or decreased wave heights at the location of the rip current with the presence of the rip channel.

Before presenting the experiments, it is helpful to discuss theoretical background governing three-dimensional circulation inside the surf zone. Primary emphasis is focused on the driving forces (torques) of the three-dimensional flows rather than the details of the hydrodynamics.

DRIVING FORCES OF THE THREE-DIMENSIONAL FLOWS

Consider a Cartesian coordinate system, where the y-axis is located at the still water line and the x-axis is directed seaward. Assuming horizontal flows, wave-induced circulation inside the surf zone is usually formulated based on depth-integrated, time-averaged continuity and momentum equations (Phillips, 1977). After neglecting the lateral shear stress coupling,

Continuity Equation

$$\frac{\partial \overline{\eta}}{\partial t} + \frac{\partial}{\partial x}[U(h+\overline{\eta})] + \frac{\partial}{\partial y}[V(h+\overline{\eta})] = 0 \tag{1}$$

Momentum Equations

$$\frac{\partial U}{\partial t} + U\frac{\partial U}{\partial x} + V\frac{\partial U}{\partial y} = -g\frac{\partial \overline{\eta}}{\partial x} + D_x + B_x \tag{2}$$

$$\frac{\partial V}{\partial t} + U\frac{\partial V}{\partial x} + V\frac{\partial V}{\partial y} = -g\frac{\partial \overline{\eta}}{\partial y} + D_y + B_y \tag{3}$$

where, t is the time, (U, V) the mean horizontal velocity components in the x- and y-direction respectively, $\overline{\eta}$ the mean water level measured from the still water level, h the still water depth, g the gravitational acceleration, and (B_x, B_y) are the shear stress components. The driving force components (D_x, D_y) are expressed in terms of the gradients of the radiation stresses.

$$D_x = -\frac{1}{\rho(h+\overline{\eta})}\left(\frac{\partial S_{xx}}{\partial x} + \frac{\partial S_{xy}}{\partial y}\right) \tag{4}$$

$$D_y = -\frac{1}{\rho(h+\overline{\eta})}\left(\frac{\partial S_{xy}}{\partial x} + \frac{\partial S_{yy}}{\partial y}\right) \tag{5}$$

in which,

$$S_{xx} = E[n(\cos^2\theta + 1) - \tfrac{1}{2}] \tag{6}$$

$$S_{xy} = E\, n \sin\theta \cos\theta \tag{7}$$

$$S_{yy} = E[n(\sin^2\theta + 1) - \tfrac{1}{2}] \tag{8}$$

where, E is the total wave energy per unit surface area and n is the ratio of the group velocity C_g to the wave celerity C.

Mean Vorticity Equations

Mean vorticity equation is obtained by cross-differentiating Equations (2) and (3) such that the set-up terms are eliminated.

$$\frac{\partial \overline{\omega}}{\partial t} + \frac{\partial}{\partial x}(U\overline{\omega}) + \frac{\partial}{\partial y}(V\overline{\omega}) = \frac{\partial D_y}{\partial x} - \frac{\partial D_x}{\partial y} + \frac{\partial B_y}{\partial x} - \frac{\partial B_x}{\partial y} \tag{9}$$

where, the mean vorticity, $\overline{\omega}$, is defined as

$$\overline{\omega} \equiv \frac{\partial V}{\partial x} - \frac{\partial U}{\partial y} \tag{10}$$

Sometimes, this time-averaged and depth-integrated vorticity equation is helpful since the contribution of set-up term to wave-induced current system is considered only indirectly through the total mean water depth $(h + \overline{\eta})$, thus making it possible to neglect $\overline{\eta}$ by assuming that $\overline{\eta}$ is small relative to the still water depth.

Vorticity Driving Torque based on Mean Vorticity Equation

The local vorticity driving torque, T_V, can be obtained directly from the mean vorticity equation presented in Equation (9):

$$T_V = \frac{\partial D_y}{\partial x} - \frac{\partial D_x}{\partial y} \tag{11}$$

in which D_x and D_y are given in Equations (4) and (5). Since D_x and D_y include the contributions by S_{xx}, S_{yy} and S_{xy}, the local torque T_V can also be expressed as the sum of three contributions: (1) $(T_V)_1$ by S_{xx}, (2) $(T_V)_2$ by S_{yy}, and (3) $(T_V)_3$ by S_{xy}.

$$T_V = (T_V)_1 + (T_V)_2 + (T_V)_3 \tag{12}$$

where,

$$(T_V)_1 = -\frac{1}{\rho(h+\overline{\eta})^2}\frac{\partial(h+\overline{\eta})}{\partial y}\frac{\partial S_{xx}}{\partial x} + \frac{1}{\rho(h+\overline{\eta})}\frac{\partial^2 S_{xx}}{\partial x \partial y} \tag{13}$$

$$(T_V)_2 = \frac{1}{\rho(h+\overline{\eta})^2}\frac{\partial(h+\overline{\eta})}{\partial x}\frac{\partial S_{yy}}{\partial y} - \frac{1}{\rho(h+\overline{\eta})}\frac{\partial^2 S_{yy}}{\partial x \partial y} \tag{14}$$

$$(T_V)_3 = \frac{1}{\rho(h+\overline{\eta})^2}\left[\frac{\partial(h+\overline{\eta})}{\partial x}\frac{\partial S_{xy}}{\partial x} - \frac{\partial(h+\overline{\eta})}{\partial y}\frac{\partial S_{xy}}{\partial y}\right] - \frac{1}{\rho(h+\overline{\eta})}\left[\frac{\partial^2 S_{xy}}{\partial x^2} - \frac{\partial^2 S_{xy}}{\partial y^2}\right] \tag{15}$$

Assuming that waves encounter the coast with nearly normal incidence (i.e., $\theta \cong \pi$), and using the shallow water asymptotes ($n = 1$), then the radiation stress terms can be written as

$$\begin{aligned} S_{xx} &= \tfrac{3}{16}\rho g H^2 \\ S_{xy} &= \tfrac{1}{8}\rho g H^2(\theta - \pi) \\ S_{yy} &= \tfrac{1}{16}\rho g H^2 \end{aligned} \tag{16}$$

Assuming further that $\overline{\eta}$ is small relative to still water depth, i.e., $(h+\overline{\eta}) \to h$ (this assumption will not be valid near the still water shoreline where $h = 0$), then vorticity driving torque components $(T_V)_1$, $(T_V)_2$ and $(T_V)_3$ can be written as follows:

$$(T_V)_1 = \frac{g}{16h}[-\frac{3}{h}\frac{\partial h}{\partial y}\frac{\partial H^2}{\partial x} + 3\frac{\partial^2 H^2}{\partial x \partial y}] \tag{17}$$

$$(T_V)_2 = \frac{g}{16h}[\frac{1}{h}\frac{\partial h}{\partial x}\frac{\partial H^2}{\partial y} - \frac{\partial^2 H^2}{\partial x \partial y}] \tag{18}$$

$$(T_V)_3 = \frac{g(\theta-\pi)}{8h}[\frac{1}{h}\frac{\partial h}{\partial x}\frac{\partial H^2}{\partial x} - (\frac{\partial^2 H^2}{\partial x^2} - \frac{\partial^2 H^2}{\partial y^2})] + \tag{19}$$

$$\frac{g}{8h}[\frac{1}{h}\frac{\partial h}{\partial x}H^2\frac{\partial \theta}{\partial x} - H^2(\frac{\partial^2 \theta}{\partial x^2} - \frac{\partial^2 \theta}{\partial y^2})] - \frac{g}{4h}[\frac{\partial \theta}{\partial x}\frac{\partial H^2}{\partial x} - \frac{\partial \theta}{\partial y}\frac{\partial H^2}{\partial y}]$$

Hence, if the distributions of wave height and local wave directions are known, the local vorticity driving torque induced on the surf zone can be calculated. It should be noted here that the torque T_V has dimensions of $[1/sec^2]$, which is not actual dimensions of torque, [force $\times$ length].

Vorticity Driving Torque based on Momentum Equations

Another expression for the vorticity driving torque, T_M, can be obtained by integrating local torque about a reference point over the entire surf zone.

$$T_M = \int\int \rho(h+\overline{\eta})[(x-x_o)D_y - (y-y_o)D_x]\, dxdy \tag{20}$$

where, (x_o, y_o) represent the coordinate of the reference point about which the total driving torque is to be calculated. Here, T_M has dimensions of torque, [force $\times$ length].

Using the radiation stress expressions given in Equation (16) with the assumption that $\overline{\eta}$ is small, T_M also can be written as the sum of three contributions: (1) $(T_M)_1$ by S_{xx}, (2) $(T_M)_2$ by S_{yy}, and (3) $(T_M)_3$ by S_{xy}, as follows:

$$T_M = (T_M)_1 + (T_M)_2 + (T_M)_3 \tag{21}$$

where,

$$(T_M)_1 = \int\int (y-y_o)\frac{\partial S_{xx}}{\partial x}dxdy = \frac{3\rho g}{16}\int\int (y-y_o)\frac{\partial H^2}{\partial x}dxdy \tag{22}$$

$$(T_M)_2 = -\int\int (x-x_o)\frac{\partial S_{yy}}{\partial y}dxdy = -\frac{\rho g}{16}\int\int (x-x_o)\frac{\partial H^2}{\partial y}dxdy \tag{23}$$

$$(T_M)_3 = \int\int [-(x-x_o)\frac{\partial S_{xy}}{\partial y} + (y-y_o)\frac{\partial S_{xy}}{\partial x}]dxdy \tag{24}$$

$$= \frac{\rho g}{8}\int\int [(y-y_o)\frac{\partial\{H^2(\theta-\pi)\}}{\partial y} - (x-x_o)\frac{\partial\{H^2(\theta-\pi)\}}{\partial x}]dxdy$$

Hence, T_M also can be calculated if the distributions of the radiation stresses, i.e., the distributions of wave heights and wave incidence angle, are known.

EXPERIMENTS

All experiments were conducted in a wave tank of the Coastal and Oceanographic Engineering Laboratory of the University of Florida. This tank is approximately 20 m long, 1.5 m high and 0.6 m wide, and is equipped with a piston type wavemaker and has glass panels on both sides of the tank. The water depth was 0.40 m in the horizontal section of the tank. Two types of regular waves of 3 cm and 9 cm heights were used while the wave period was fixed at 1.43 sec during the experiments. The bathymetry was configured to represent a bar morphology by superimposing two-dimensional and three-dimensional wood bars parallel to the coast on a uniform slope of 1:20. The two-dimensional bar extended to the whole width of the tank, while the three-dimensional bar extended from one wall to two-thirds of the tank width. These bars were installed approximately at the surf line, which depends on wave height condition. All four tests (two waves and two bars) were carried out to document the wave heights and wave direction distribution within and adjacent to the surf zone. The details are described in Oh (1994).

Wave hights and direction fields were measured to document and interpret the interaction of the waves and bar-induced currents. Figures 1 and 2 present the isolines of wave heights in the presence of the three-dimensional bar for the small waves and for the large waves, respectively. For the small waves, as shown in Figure 1, wave crest lines were almost uniform in the longshore direction even in the presence of the three-dimensional bar, which implied that the return flow due to the three-dimensional bar was weak to modify the wave fields. It is seen from Figure 2 that waves were much higher in the vicinity of the seaward return flow than those near the bar area. Much higher waves appeared to be caused by increased return current induced by the three-dimensional bar. However, it should be noted that the breakerline was not significantly influenced by the return flow. [It was observed by Dean and Oh (1994) that the breakerline was significantly displaced seaward near the return current during the circulation tests with the jet present on a prismatic beach.] Uniform breakerline with the three-dimensional bar morphology appeared to be due to both relatively weak return current induced by the three-dimensional bar and deeper water depth at the return current area than the area over the bar, and it was agreed with the field observations by Sonu (1972).

RESULTS AND DISCUSSIONS

Vorticity Driving Torque based on Mean Vorticity Equation

Considering that waves encounters the coast with normal incidence ($\theta = \pi$), Equations (17), (18), and (19) can be expressed as the combinations of different individual components depending on the wave height gradients and water depth near the bar area, as follows:

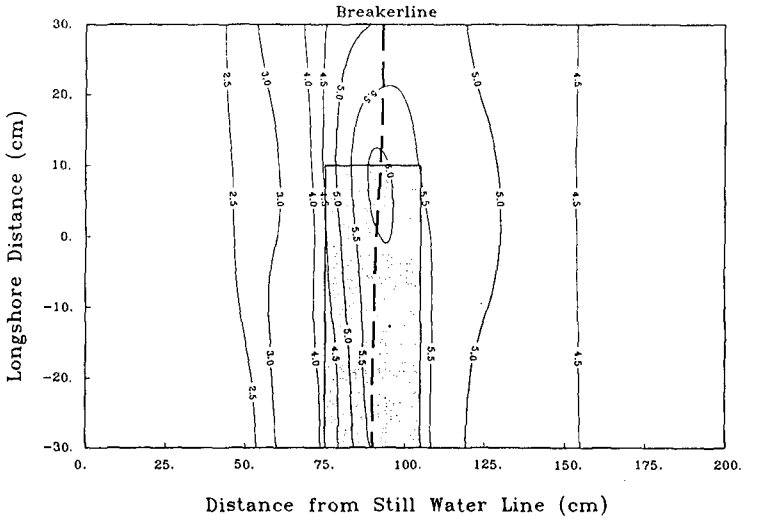

Figure 1: Wave Height Distributions in the Presence of Three-Dimensional Bar when $H_o = 3cm$. Wave heights are given in cm. A dark area represents the area covered by the three-dimensional bar. Note that wave fields are not greatly influenced by the return flow induced due to the presence of the three-dimensional bar, resulting in more or less uniform breakerline.

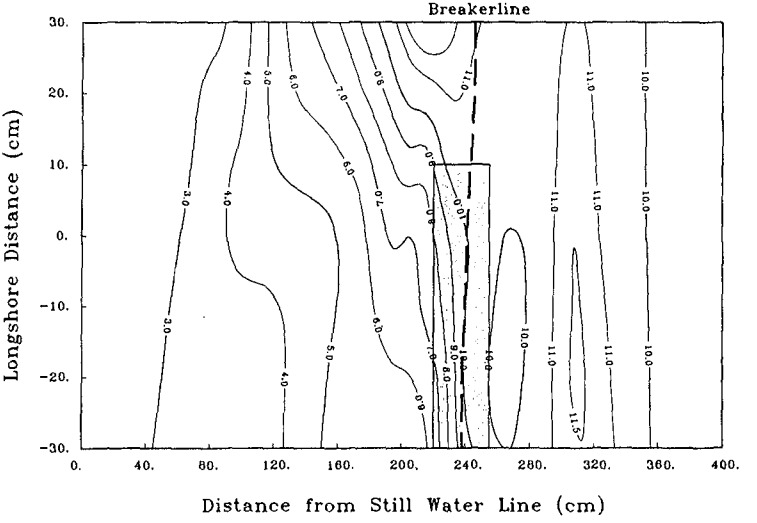

Figure 2: Wave Height Distributions in the Presence of Three-Dimensional Bar when $H_o = 9cm$. Wave heights are given in cm. A dark area represents the area covered by the three-dimensional bar. Note that wave fields are substantially influenced by the return flow induced due to the presence of the three-dimensional bar. Note also almost uniform breakerline due to deeper water depth at the area of return flow than the area over the bar.

$$\begin{aligned} (T_V)_1 &= 3\ (II - VI) \\ (T_V)_2 &= I - II \\ (T_V)_3 &= 0 \end{aligned} \tag{25}$$

where,

$$I = \frac{g}{16h^2}\frac{\partial h}{\partial x}\frac{\partial H^2}{\partial y} \tag{26}$$

$$II = \frac{g}{16h}\frac{\partial^2 H^2}{\partial x \partial y} \tag{27}$$

$$VI = \frac{g}{16h^2}\frac{\partial h}{\partial y}\frac{\partial H^2}{\partial x} \tag{28}$$

The marginal distributions of individual components are presented in Figure 3 for the large waves. When the three-dimensional bar is installed, the vorticity driving torque is mainly contributed by Component VI, which includes the gradients of water depth in the y-direction, $\frac{\partial h}{\partial y}$, and is confined in the vicinity of the three-dimensional bar area. With the two-dimensional bar present, in which case $\frac{\partial h}{\partial y}$ is zero, the magnitude of the Components I and II are negligible. It is noted for the large wave tests in the presence of the three-dimensional bar that Component I increases up to a comparable magnitude to Component VI, as shown in Figure 3(b). This effect might be due to the increase in the gradients of wave heights in the y-direction. Due to space limitations, the results for the small wave condition will not be presented here; however, it was found that the results were consistent with those for the large waves.

The marginal distributions of the total torque are shown in Figure 4 for the large wave condition in the presence of the three-dimensional bar. Positive circulations occur within the surf zone and in the area seaward of the bar region but the magnitudes of these circulations are smaller than and overshadowed by the negative circulation near the bar area. Hence, it would be necessary for future experiments to simulate the more realistic and smooth bar morphology which could avoid these exaggerated effects of the depth gradients in the y-direction. However, these results clearly demonstrate that rip currents are stable on a three-dimensional barred beach although increased momentum fluxes of waves in the area with opposing currents induced by the bar tend to work against rip currents. It appeared that the water mass transported over the bar tended to return to offshore through deeper area in the bar morphology.

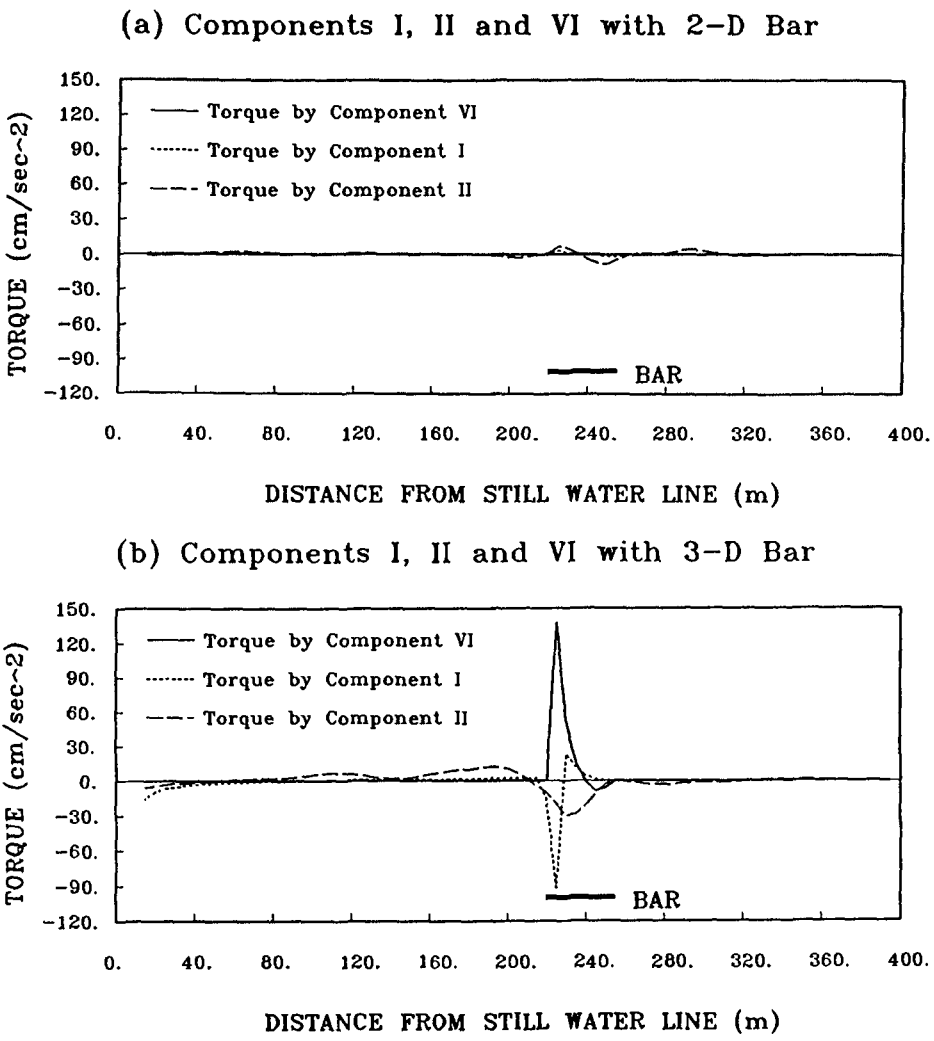

Figure 3: Marginal Distributions of Individual Components along x-axis in cm/sec^2 when $H_o = 9cm$: (a) Components I, II and VI in the presence of the two-dimensional (2-D) bar and (b) Components I, II and VI in the presence of the three-dimensional (3-D) bar

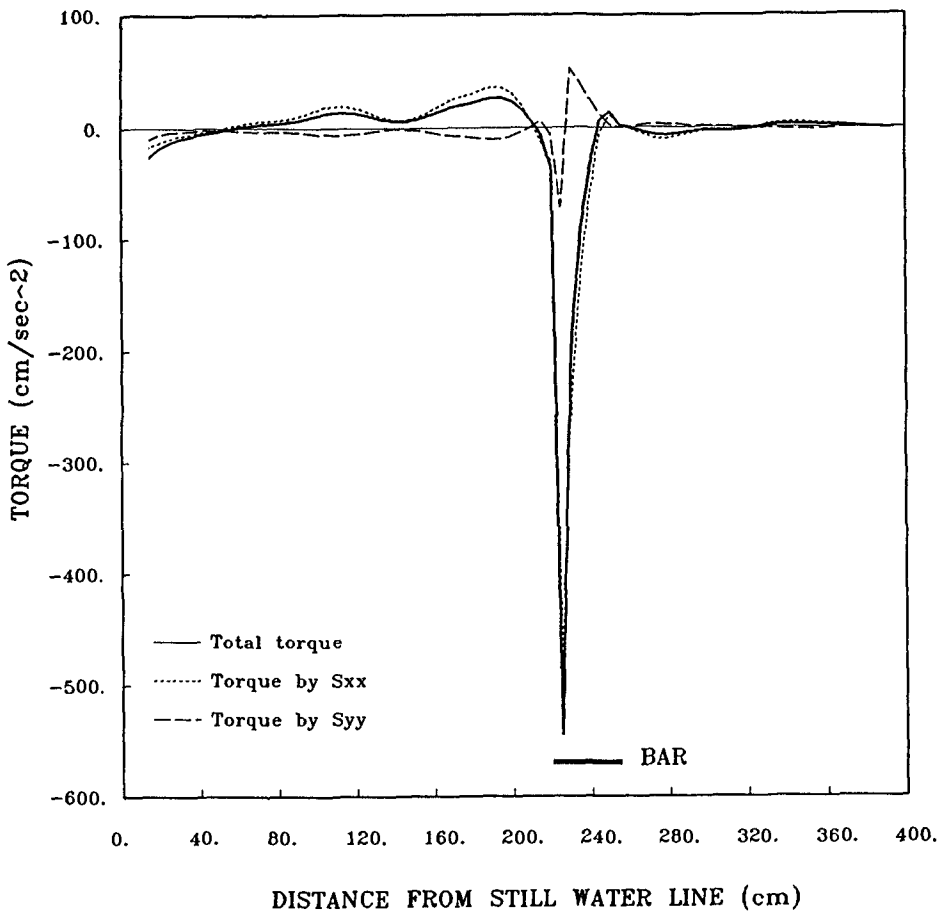

Figure 4: Marginal Distributions of Total Torque and the Contributions of Radiation Stresses Components along x-axis in cm/sec^2 when $H_o = 9cm$ in the Presence of the Three-Dimensional Bar. Note that torque by S_{xx} is dominant over the torque contributed by S_{yy}. Note also the positive values within the surf zone and in the area seaward of the bar. Hence, positive circulation occurs within the surf zone, which tends to suppress the bar-induced circulation.

Vorticity Driving Torque based on Momentum Equation

Marginal distributions of the total torque and the contributions by S_{xx} and S_{yy} were calculated based on the momentum equations, as presented in Equations (21) to (24), and the results are presented in Figure 5 for the large waves ($H_o = 9cm$) in the presence of the three-dimensional bar. For these calculations, the reference point was selected as the centerline point at the same x-location as the location of the bar crest. The contribution by S_{yy} dominates over the contribution by S_{xx} within the whole area of interest except the area over the bar, where the contribution by S_{xx} is dominant since $(x - x_o)$ is small in this area. The total torque changes from negative values near the shoreline to positive values within the surf zone and again to negative values over the bar, and demonstrates oscillating patterns beyond the breakerline. This figure clearly exhibits the opposing effects of waves to the bar-induced circulation, thus tending to stabilize the surf zone.

Table 1 summarizes the total torque induced on the area of interest from the shoreline to offshore. The positive values of the total torque T_M demonstrate that the wave-induced torque is in opposition to the three-dimensional bar-induced circulation (flowing from the bar area, i.e. shoals, to the base of return current, i.e. the embayments). The opposing wave effects appeared to be due to the increased momentum fluxes associated with higher waves in the vicinity of the return flow.

Table 1: Summary of Total Vorticity Driving Torque based on the Momentum Equation.

Item	Unit	$H_o = 3cm$		$H_o = 9cm$	
		2-D Bar	3-D Bar	2-D Bar	3-D Bar
$\sum\sum D_x$	N	-0.98	-1.29	-8.08	-8.40
$\sum\sum D_y$	N	0.049	0.011	0.23	-4.04
$(T_M)_1$ by S_{xx}	$N-m$	-0.002	-0.005	-0.001	0.035
$(T_M)_2$ by S_{yy}	$N-m$	0.015	0.036	0.376	1.103
Total torque, T_M	$N-m$	0.013	0.031	0.375	1.138

SUMMARY AND CONCLUSIONS

A series of fixed bed tests was carried out to investigate the generation and existence of three-dimensional flows on a barred beach. The bar morphology represented periodic forms parallel to the coast superimposed on a linear sloping beach. For these tests, wave heights and wave direction fields within and adjacent to the surf zone were documented to calculate the wave-induced horizontal torque.

It was found for the large wave condition ($H_o = 9cm$) that three-dimensional circulations occurred due to the effect of the three-dimensional bar morphology and flowed from the bar area (shoals) to the return channel (embayments), thus

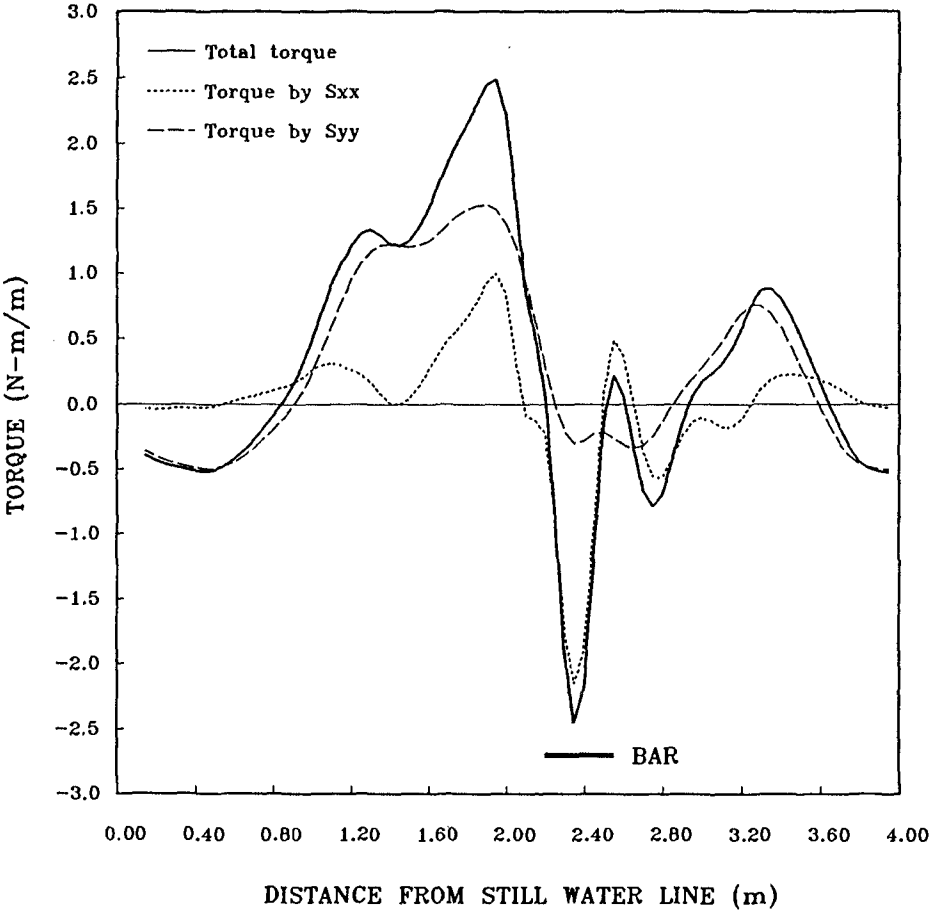

Figure 5: Marginal Distributions of Total Torque and the Contributions of Radiation Stresses Components based on Momentum Equations along x-axis in $N-m/m$ when $H_o = 9cm$ with the Three-Dimensional Bar. Note that the contribution by S_{yy} is dominant term over the whole area of interest except over the bar area, where the contribution by S_{xx} is dominant. Positive circulation occurs within the surf zone, resulting in opposing effects of waves on the three-dimensional bar-induced circulation.

modifying the wave fields such that waves were higher in the vicinity of the return current. However, the breakerline was not significantly influenced by the return flow since the return current induced by the three-dimensional bar was weak and the water depth in the vicinity of the return current was deeper than that in the area over the bar, which was agreed with the field observations.

When waves were small ($H_o = 3cm$), the resulting circulation pattern was the same as that for the large waves; however, the circulation was too weak to modify the wave fields. These results could indicate that rip currents need the wave height larger than a lower limit to form even with the bar morphology, which was observed in the field.

When individual components of the vorticity driving torque was calculated based on the mean vorticity equation, the component which included the depth gradients in the longshore direction demonstrated the largest contribution.

The marginal distributions of the total torque for the large wave tests with the three-dimensional bar present show positive circulations within the surf zone and in the area seaward of the bar region; hence, these results clearly demonstrated that rip currents were stable on three-dimensionally barred beach although increased momentum fluxes of waves in the area with opposing currents induced by the bar tended to exert a counter force against them. It appeared that the water mass transported over the bar tended to return to offshore through deeper area in the bar morphology, where the depth gradients in the longshore direction existed.

When the vorticity driving torque was calculated based on the momentum equations for the large wave condition tests in the presence of the three-dimensional bar, the contribution by S_{yy} dominated over the contribution by S_{xx} within the whole area of interest except the area over the bar. The total torque changed from negative values near the shoreline to positive values within the surf zone, which clearly demonstrated the opposing effects of waves to the bar-induced circulation, thus tending to stabilize the surf zone. The opposing wave effects appeared to be due to the increased momentum fluxes associated with higher waves in the vicinity of the return flow.

In aggregate, these studies suggest that rip currents are stable on three- dimensionally barred beach although increased momentum fluxes of waves in the area with opposing currents induced by the bar tended to exert a counter force against them. It appeared that the water mass transported over the bar tended to return to sea through deeper area in the bar morphology. This cause is believed to be due to the greater hydraulic efficiency of flows through deeper portions of the profile, which leads to a hydraulic/sedimentary instability which causes development of a vestigial channel.

REFERENCES

Bowen, A.J. (1969), "Rip Currents. Part 1: Theoretical Investigation", J. of Geophysical Research, Vol. 74, No. 23, pp. 5467-5478.

Bowen, A.J. and D.L. Inman (1969), "Rip Currents. Part 2: Laboratory and Field Observations", J. of Geophysical Research, Vol. 74, No. 23, pp. 5479-5490.

Dalrymple, R.A. (1975), "A Mechanism for Rip Current Generation on an Open Coast", J. of Geophysical Research, Vol. 80, No. 24, pp. 3485-3487.

Dalrymple, R.A. and C.J. Lozano (1978), "Wave-Current Interaction Models for Rip Currents", J. of Geophysical Research, Vol. 83, No. C12, Paper No. 8C0556, pp. 6063-6071.

Dean, R.G. and T.M. Oh (1994), "Three-Dimensional Morphology in a Narrow Wave Tank: Measurement and Theory", Proc. 24th Int. Conf. on Coastal Eng., Kobe, Japan, ASCE

Deigaard, R. (1990), "The Formation of Rip Channels on a Barred Coast", Progress Report No. 72, Institute of Hydrodynamics and Hydraulic Eng., ISVA, Tech. Univ. Denmark, pp. 65-74.

Gourlay, M. R. (1976), "Non-Uniform Alongshore Currents", Proc. 15th Int. Conf. on Coastal Eng., Honolulu, Hawaii, ASCE, pp. 701-720.

Hino, M. (1974), "Theory on Formation of Rip-Current and Cuspidal Coast", Proc. 14th Int. Conf. on Coastal Eng., Copenhagen, Denmark, ASCE, pp. 901-919.

Oh, T.M. (1994), "Three-Dimensional Hydrodynamics and Morphology Associated with Rip Currents", Ph.D. Dissertation, Dept. of Coastal and Oceanographic Eng., Univ. of Florida, Gainesville, Florida, 210 pp.

Phillips, O.M. (1977), "The Dynamics of the Upper Ocean", Cambridge Univ. Press, New York, 363 pp.

Sonu, C.J. (1972), "Field Observation of Nearshore Circulation and Meandering Currents", J. of Geophysical Research, Vol. 77, No. 18, pp. 3232-3247.

Wind, H.G. and C.B. Vreugdenhil (1986), "Rip-Current Generation near Structures", J. of Fluid Mech., Vol. 171, pp. 459-476.